The reactivity of spectroscopically detected peroxy complexes of iron porphyrins

Alan L. Balch
Department of Chemistry, University of California, Davis, CA 95616 (USA)

Abstract
The coordination of alkyl peroxides by heme proteins is an important step in the functioning of several enzymes, (for example, peroxidases, cytochrome P_{450}, estrogen synthase). Generally the reaction of peroxides with iron porphyrins in the absence of a proton results in the destruction of both porphyrin and peroxide. However, three distinct intermediates involving coordination of peroxides to iron porphyrins can be identified using spectroscopic techniques. The formation, spectroscopic characteristics and chemical behavior of these reactive intermediates are reviewed here.

Introduction

Iron complexes of peroxides are implicated in the activity of a number of enzymes that utilize either peroxides or dioxygen as substrates. The peroxidases are a large group of enzymes which react with hydrogen peroxide or alkyl peroxides to oxidize a wide range of substrates [1, 2]. Two intermediates, green compound **I** and red compound **II**, are directly detected in the functioning cycle of horseradish peroxidase which is shown in Scheme 1, which emphasizes recent information regarding the hydrogen bonding network within the active site [3]. Both intermediates contain the ferryl $(Fe^{IV}=O)^{2+}$ moiety. In compound **I**, the porphyrin is also oxidized to a radical state. The early stage where the peroxide itself interacts with the heme is not sufficiently long lived for direct spectroscopic detection. However, there is recent evidence from low-temperature, stopped flow experiments for the formation of another intermediate, compound **O**, whose formation appears to precede that of compound **I** [4]. The structure of this intermediate and the cause for its hyperporphyrin absorption spectrum with a split Soret peak remain to be established.

Cytochrome P-450 activates dioxygen for the hydroxylation of hydrocarbons. A generally accepted cycle for its operation is shown in Scheme 2 [5–7]. In this cycle, dioxygen or a peroxide can serve as the oxidant. The intermediate **A** which is obtained by reduction of the dioxygen adduct is generally formulated as an iron(III) complex with an axially coordinated peroxide. A coordinated peroxide model has also been proposed in the conversion of androgen to estrogens by a P-450 enzyme, estrogen synthetase (aromatase) [8].

As these examples show, the interaction of iron complexes with hydrogen peroxide and alkyl peroxides have critical importance in heme enzyme chemistry. However, in model systems it is well recognized that

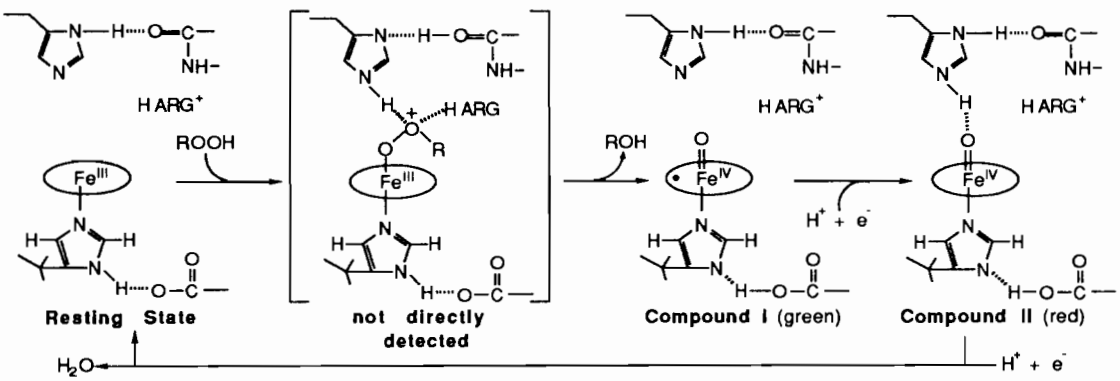

Scheme 1. Catalytic cycle for horseradish peroxidase.

0020-1693/92/$5.00

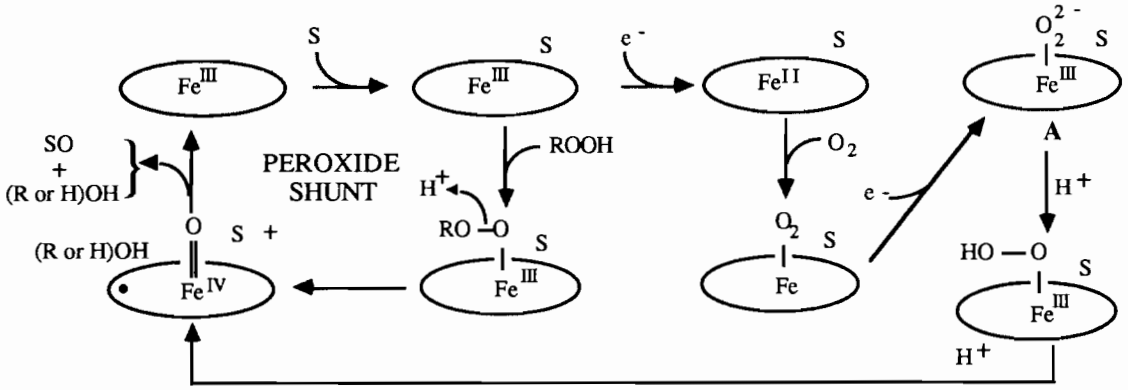

S is the substrate, SO is its oxygenated form.

Scheme 2. Catalytic cycle for cytochrome P-450.

the iron porphyrin/hydroperoxide reaction is one that frequently destroys both the porphyrin and the peroxide [9]. Only in recent years has it become possible to detect directly simple, synthetic iron porphyrin complexes with peroxide ions as axial ligands through spectroscopic techniques. Much of this work, particularly the study of chemical reactivity, has relied upon ^1H and ^2H NMR spectroscopy to detect and follow the key iron complexes. The advantages of the wide dispersal of the NMR resonances of paramagnetic iron porphyrins has been reviewed in several articles [10–12].

Here the chemical behavior of three iron porphyrin peroxide intermediates that have been detected is reviewed. Abbreviations used and the iron(II) porphyrin structure are given below. The extensive and complex literature [13, 14] which surrounds kinetic studies of the reactions of peroxides with iron porphyrins is outside the scope of this article.

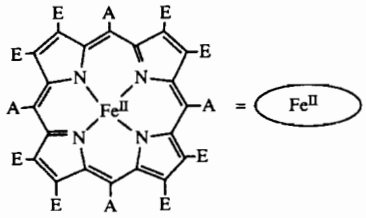

Iron(II) Porphyrin

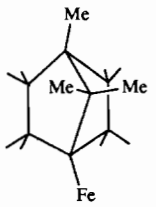

4-camphane (4-cam) axial ligand

Abbreviations Used

P, generic porphyrin dianion

TPP, Tetraphenylporphyrin dianion; A = Ph, E = H

TmTp, Tetra(*m*-tolyl)porphyrin dianion; A = *m*-$CH_3C_6H_4$, E = H

TMP, Tetramesitylporphyrin dianion; A = 2,4,6 trimethylphenyl, E = H

OEP, Octaethyl porphyrin dianion; A = H, E = C_2H_5

R, Alkyl or Aryl Group

py, pyridine

N-MeIm, N-methyl imidazole

The dinuclear peroxo-bridged intermediate, PFe^{III}–O–O–$Fe^{III}P$

Treatment of four-coordinate iron(II) porphyrins with dioxygen in non-polar, non-coordinating solvent leads to the formation of the stable, isolable μ-oxo species, PFe^{III}–O–$Fe^{III}P$, via the sequence of detectable intermediates shown in Scheme 3 [14, 15]. The second intermediate, the μ-peroxo complex, PFe^{III}–O–O–$Fe^{III}P$, is the subject of this section. Spectroscopic properties which serve to characterize this intermediate are given in Table 1 [15–21]. This table also contains information on the μ-oxo species PFe^{III}–O–$Fe^{III}P$. The μ-peroxo and μ-oxo complexes are similar in that both contain two iron(III) ions which are antiferromagnetically coupled. Both dinuclear complexes have magnetic moments that increase with increasing temperature and ^1H NMR spectra that deviate markedly from Curie law behavior. The larger magnetic moment for the peroxo bridged dimer indicates that the antiferromagnetic coupling in it is smaller in absolute value than that in the oxo bridged dimers (which typically have $J \sim -130\ cm^{-1}$) [21]. The patterns of the ^1H NMR spectra of the two species are also closely similar and quite distinct from high-spin, five-coordinate iron(III) porphyrin monomers. These monomers show large downfield shifts (*c.* 110 pm at −70 °C) for the pyrrole protons [10–12].

PFe^{III}–O–O–$Fe^{III}P$ is readily formed when dioxygen is added to unhindered iron(II) porphyrins at −70 °C in toluene [15, 16]. These reactions are easily followed by ^1H NMR spectroscopy. Figure 1 shows the spectrum of a specifically prepared mixture containingTmTPFe^{II}, TmTPFe^{III}–O–O–Fe^{III}TmTP, and TmTPFe^{III}–O–Fe^{III}TmTP taken with at 100 MHz [15]. Resonances of each component were readily distinguishable even at this low field. Toluene solutions containing only PFe^{III}–O–O–$Fe^{III}P$ can be prepared.

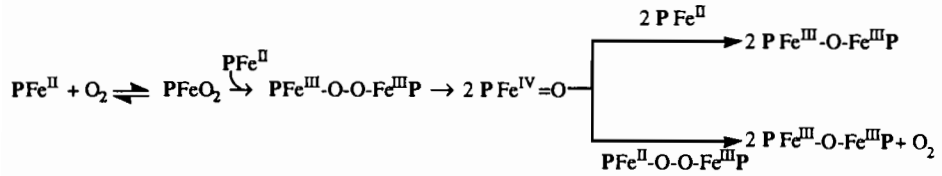

Scheme 3. Reactions of PFe^{II} with dioxygen in a non-coordinating environment.

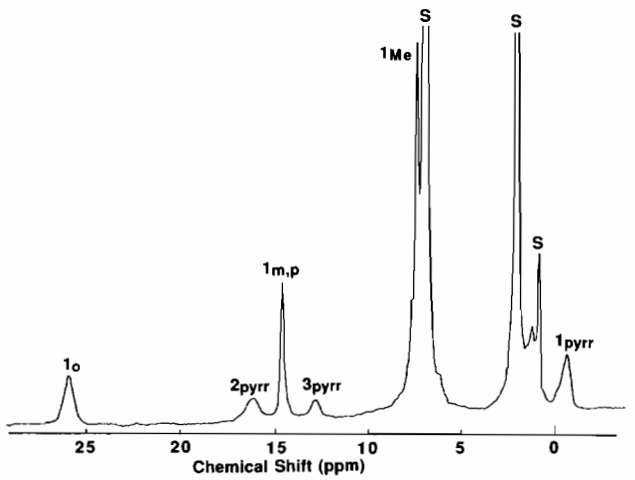

Fig. 1. 100 MHz ^{1}H NMR spectrum of a toluene-d_8 solution containing: 1, TmTPFe^{II}; 2, TmTPFe^{III}–O–O–Fe^{III}TmTP; 3, TmTPFe^{III}–O–Fe^{III}TmTP at −50 °C. The subscripts identify the pyrrole resonances as pyrr, the *ortho*, *meta* and *para* phenyl resonances as o, m, and p and the methyl resonance as Me. Resonances labeled S arise from the solvent and impurities in it. Adapted from ref. 15 and reprinted with permission, copyright 1977 Am. Chem. Soc.

These are stable indefinitely at −70 °C but decompose in a matter of minutes at −30 °C. Attempts to remove dioxygen from solutions of the peroxide bridged complex were unsuccessful. Hence, its formation at −70 °C is irreversible. On warming, however, dioxygen is released stoichiometrically in accord with reaction (1). When PFe^{III}–O–O–Fe^{III}P is formed from a mixture of $^{18}O_2$ and $^{16}O_2$ and then allowed to react via eqn. (1),

$$2\mathbf{P}Fe^{III}\text{–O–O–}Fe^{III}\mathbf{P} \longrightarrow 2\mathbf{P}Fe^{III}\text{–O–}Fe^{III}\mathbf{P} + O_2 \qquad (1)$$

the isotopic composition of the dioxygen evolved shows that no $^{16}O^{18}O$ is formed [16]. Thus the O–O bond cleavage step involved in reaction (1) is irreversible. The process involves initial homolysis of one peroxo bridged dimer to generate two ferryl complexes, PFe^{IV}=O. These then attack the back side of intact peroxo bridge dimers to liberate PFe^{II}, dioxygen and the μ-oxo dimer. At 251 K, the rate of reaction (5) is independent of dioxygen concentration and first order in the concentration of PFe^{III}–O–O–Fe^{III}P with a rate constant 0.035(3) min^{-1}. Activation parameters are $\Delta G^{\ddagger} = 19(1)$ kcal/mol, $\Delta H^{\ddagger} = 14.5(1)$ kcal/mol and $\Delta S^{\ddagger} = -15(1)$ eμ.

PFe^{III}–O–O–Fe^{III}P is surprisingly unreactive as an oxidant. This is probably because the peroxide bridge is buried between the two metalloporphyrin units and therefore protected from encountering suitable substrates. At −70 °C, PFe^{III}–O–O–Fe^{III}P does not react with diethyl sulfide, *t*-butyl mercaptan or triphenylphosphine [22]. In fact, this dimer can even be formed from PFe^{II} and dioxygen in the presence of an excess of triphenylphosphine at low temperature. However, when warmed above −70 °C, PFe–O–O–Fe^{III}P does undergo reaction with triphenylphosphine to produce PFe^{II} and triphenylphosphine oxide. This occurs through initial homolysis of the O–O bond in the peroxide bridged dimer to form the ferryl complex, PFe^{IV}=O, which is the actual oxidant. Kinetic studies, which show that the rate of loss of PFe^{III}–O–O–Fe^{III}P is slowed by a factor of one half in the presence of triphenylphosphine, are consistent with the intermediacy of the ferryl intermediate in this oxidation. This lowering of the rate occurs because the cleavage of one O–O bond in PFe^{III}–O–O–Fe^{III}P results in the eventual destruction of two molecules of PFe^{III}–O–O–Fe^{III}P when no other substrate is present. However, when triphenylphosphine is present, it acts to protect unreacted PFe^{III}–O–O–Fe^{III}P by reacting with the ferryl intermediate, PFe^{IV}=O. As a result, iron(II) porphyrins are good catalysts for triphenylphosphine oxidation via the cycle showing in Scheme 4.

Despite its low reactivity toward triphenylphosphine, PFe^{III}–O–O–Fe^{III}P is subject to reactions with amines even at −70 °C [17, 23–25]. Addition of piperidine, pyridine or *N*-methyl imidazole (collectively, **B**) occurs stoichiometrically according to eqn. (2). The red, paramagnetic ($S = 1$) ferryl complexes that result are

$$2\mathbf{B} + Fe^{III}\text{–O–O–}Fe^{III}\mathbf{P} \longrightarrow 2(\mathbf{B})Fe^{IV}\text{=O} \qquad (2)$$

also sufficiently stable at −70 °C so that they can be directly observed through a variety of spectroscopic techniques. Notice that the order of addition of reagents here is necessary to form the peroxo and ferryl complexes. Only when the base is added after dioxygen

TABLE 1. Spectroscopic properties of peroxo and oxo bridged iron porphyrin

	T (°C)	$TmTPFe^{III}$–O–O–$Fe^{III}TmTP$	Reference	$TmTPFe^{III}$–O–$Fe^{III}TmTP$	Reference
^1H NMR	50	pyrrole, 16 ppm; phenyl-H, −7.9 ppm	15, 16	pyrrole, 13 ppm; phenyl-H, −7.9 ppm	16, 20
	−70	(*meso*, −2.5; methylene, 8.7, 6.3)[a]	17		
Magnetic moment	−50	2.6 μ_B	15, 16	1.5 μ_B	16, 21
EPR	−196	none observed	15, 16	none reported	21
UV–Vis: λ_{max} (nm) ($\epsilon(M^{-1}\ cm^{-1})$)	−80	630(5.0×10^3), 540(1.8×10^4)	15, 16	606(1.0×10^4), 565(2.0×10^4)	15, 16
Mössbauer[b]	−196[a]	δ, 0.54 mm/s; ΔE, 0.79 mm/s	18	δ, 0.40 mm/s; ΔE, 0.60 mm/s	18
Raman		photolabile	19		

[a]Ligand is etioporphyrin III. [b]Ligand is tetraphenylporphyrin.

Scheme 4. Catalytic oxidation of triphenylphosphine [22].

has reacted is it possible to observe the successive formation of PFe^{III}–O–O–$Fe^{III}P$ and (B)PFe^{IV}=O.

Sulfur dioxide is oxidized at −70 °C by PFe^{III}–O–O–$Fe^{III}P$ as shown in eqn. (3) [26]. Whether this occurs by direct attack of sulfur dioxide on the peroxide link or whether sulfur dioxide acts

$$SO_2 + PFe^{III}\text{–O–O–}Fe^{III}P \longrightarrow PFe^{III}O_2SO_2Fe^{III}P \quad (3)$$

first as a base to generate a reactive ferryl complex via eqn. (2) and then this ferryl complex oxidizes SO_2 remains to be seen.

The formation of the peroxo bridge in PFe^{III}–O–O–$Fe^{III}P$ is subject to steric constraints. Tetra(aryl)porphyrins bearing suitably sized substituents in the *ortho* or *meta* aryl positions may be too hindered to allow the approach of the two porphyrins that is required to form this bridge. Thus addition of dioxygen to iron(II) porphyrins with substituents protruding on both sides of the porphyrin plane stops at the first step of Scheme 3 to form $PFeO_2$ [27]. These five-coordinate dioxygen adducts can be observed so long as the sample is maintained at low temperature. This occurs when the porphyrin is tetra-(2,4,6-tri(ethoxy)phenyl)-porphyrin, tetra-(2,4,6-tri(methoxy)phenyl)porphyrin or tetra-(3,4,5-tri(methoxy)phenyl)porphyrin. The dioxygen adducts have been detected in ^1H NMR studies, which reveal that they are diamagnetic [27], and by Raman studies in toluene solution at low temperatures [19].

The reactivity of $TMPFe^{II}$ with dioxygen allows both $TMPFeO_2$ and $TMPFe^{III}$–O–O–$Fe^{III}TMP$ to be detected [19, 24]. Oxygenation of $TMPFe^{II}$ at −100 °C in toluene solution produces $TMPFeO_2$ which has been observed by Raman spectroscopy [19]. Warming such a sample to −70 °C or adding dioxygen to $TMPFe^{II}$ at −70 °C results in the formation of $TMPFe^{III}$–O–O–$Fe^{III}TMP$. This has been detected by both ^1H NMR and UV–Vis spectroscopy [24]. The peroxo bridged complex is extremely photolabile and a poor Raman scatterer [19]. Consequently, no Raman spectrum for the peroxide bridged species is available. Previous work purporting to report the Raman spectrum of $TMPFe^{III}$–O–O–$Fe^{III}TMP$ should be viewed with

caution due to problems of sample purity and photolability [28, 29].

The anionic mononuclear iron peroxide complex, $[PFe^{III}O_2]^-$

The anionic complexes, $[PFe^{III}O_2]^-$, which are sufficiently stable so that they can be prepared at room temperature, have been obtained by three independent means. These include treatment of $PFe^{III}Cl$ or PFe^{II} with superoxide [30–33], addition of dioxygen to $[PFe^{I}]^-$ [34], and reduction of the dioxygen complex $PFeO_2$ [35] as shown in Scheme 5. These reactions are generally performed in acetonitrile or dimethyl sulfoxide solution. It is not known whether these solvents are bound in the axial coordination site opposite the bound peroxide. However, the most obvious route to form $[PFe^{III}O_2]^-$, treatment of an iron(III) porphyrin directly with peroxide dianion, has not proven to be a suitable means of obtaining these species [35]. This failure is caused by the high basicity of the peroxide dianion which attacks the solvent (dimethyl sulfoxide) and leads to reduction of the iron to form PFe^{II} and $[PFe^{I}]^-$ rather than $[PFe^{III}O_2]^-$.

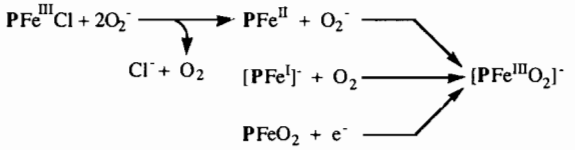

Scheme 5. Routes to the formation of $[PFe^{III}O_2]^-$.

The physical characteristics of representative examples of these anionic complexes are given in Table 2. The ^1H NMR spectrum of the anion is too broad for observation. Consequently the species was characterized by ^2H NMR on selectively deuterated samples [34]. The pattern of resonances is consistent with a high-spin, five-coordinate iron(III) formulation. Similarly the Mössbauer parameters are also indicative of a high-spin iron(III) species. The EPR spectrum, however, is distinctive and clearly different from most high-spin, five-coordinate porphyrins which show an intense signal at $g=6$ with a weak feature at $g=2$. In the case of $[PFe^{III}O_2]^-$, the spectrum is dominated by a $g=4$ resonance with much weaker features at $g \cong 9$ and $g \cong 2$. The spectrum is characteristic of rhombic iron(III) complexes and the EPR spectrum serves as a distinctive marker of this peroxide complex.

While $[PFe^{III}O_2]^-$ is sufficiently stable so that it can be isolated as a solid salt [32], crystals suitable for X-ray diffraction have not been obtained. However, structural data are available from an EXAFS study [37]. In order to obtain information regarding the iron/peroxide bonding, a perturbed difference Fourier analysis was performed that compared data from $[TPPFe^{I}]^-$ and $[TPPFe^{III}O_2]^-$. This analysis indicated that the peroxide was bound to iron in a side-on fashion with a $Fe\cdot\cdot O_2$ distance of 1.80(3) Å and the iron displaced at least 0.2(1) Å from the plane of the porphyrin [37]. This structure corresponds to that seen by X-ray crystallography for $PTi^{IV}O_2$ [38] and $[PMn^{III}O_2]^-$ [39]. The structure of the latter is shown in Fig. 2.

The reactivity of $[PFe^{III}O_2]^-$ deserves particular attention since it is a model for **A**, one of the presumed reactive complexes in the catalytic cycle of cytochrome P-450 (see Scheme 2). However, $[PFe^{III}O_2]^-$ itself appears to be a rather ineffective oxidant. It does not epoxidize styrene [35]. It is capable of oxidizing triphenylphosphine, but the yields of triphenylphosphine oxide are low (*c.* 16% in tetrahydrofuran, 31% in dimethylacetamide) [36]. There are no published reports documenting the conversion of $[PFe^{III}O_2]^-$ into a ferryl complex. This is a key step in the proposed catalytic cycle (Scheme 2) of cytochrome P-450 and further efforts to accomplish this transformation in a model system are worthwhile.

Iron(III) porphyrin complexes of alkyl peroxides, $PFe^{III}OOR$

Alkyl peroxide complexes of iron porphyrins can be obtained by two routes: the addition of dioxygen to low-spin (*S*-1/2), five-coordinated alkyl complexes of

TABLE 2. Spectroscopic properties of $[PFe^{III}O_2]^-$

	$[TPPFe^{III}O_2]^-$	Reference	$[OEPFe^{III}O_2]^-$	Reference
^2H NMR (28 °C)	pyrrole-D, 60 ppm	33		
Magnetic moment (25 °C)	$\geqslant 5.6\ \mu_B$	31	5.75 μ_B	32
EPR (g) (−196 °C)	8, 4.2, ~2	31	9.5, 4.2, ~1.3	32
UV–Vis: λ_{max} (nm) (ϵ (M^{-1} cm^{-1}))	609, 595(sh), 565, 548(sh), 437	31	530 ($6–7\times10^3$), 543 (9×10^3), 569 (8×10^3), 582sh (6×10^3)	32
Mössbauer	δ, 0.57 mm/s; ΔE, 1.0 mm/s	32	δ, 0.67 mm/s; ΔE, 0.62 nm/s	32
IR, ν(OO)			806 cm^{-1}	32

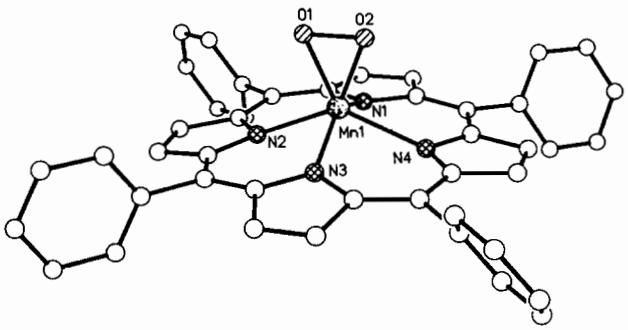

Fig. 2. The structure of the anion $[TPPMn^{III}O_2]^-$, a model for $[PFe^{III}O_2]^-$, in [K(K222)][$TPPMn^{III}O_2$]. The Mn–O bond lengths are nearly equal (1.901(4) and 1.888(4) Å) and the manganese ion is 0.641 Å out of the N_4 plane. Redrawn from coordinates from ref. 39.

iron porphyrins (eqn. (4)) [40–42] or by the addition

$$PFe^{III}R + O_2 \longrightarrow PFe^{III}\text{–}O\text{–}O\text{–}R \qquad (4)$$

$$PFe^{III}OH + HOOR \longrightarrow PFe^{III}\text{–}O\text{–}O\text{–}R + H_2O \qquad (5)$$

of an alkyl hydroperoxide to a porphyrin iron(III) hydroxy complex (eqn. (5)) [41, 43]. When the alkyl groups R in eqns. (4) and (5) are the same and the same porphyrin is employed, identical intermediates are formed. Complexes of the PFe^{III}–O–O–R type are exceedingly unstable and have only been detected in toluene solution at low temperatures (< -70 °C). Even then they form part of a mixture, for invariably their formation and decomposition occur at similar rates. As a consequence, less physical data are available for these intermediates than for either of the other two types previously described in this article. A third potential route to these intermediates, the alkylation of the anionic peroxide complex, $[PFe^{III}O_2]^-$ which was described in the preceding section, deserves to be examined.

The principle means of detection of PFe^{III}–O–O–R has been ^1H and ^2H NMR spectroscopy at low temperature. Figure 3 shows relevant ^1H NMR spectra that demonstrate formation of the intermediate via the dioxygen insertion route, eqn. (4) [41]. Trace A shows the ^1H NMR spectrum of $TTPFe^{III}C_2H_5$ with its characteristic sharp, upfield pyrrole and methyl (β) resonances. Upon addition of dioxygen (trace B) at -80 °C, two new broad resonances appear at *c.* 120 ppm. This is the region characteristic for the pyrrole protons of high-spin, five-coordinate iron(III) porphyrins. The species ($TPPFe^{III}$–O–O–C_2H_5) that is responsible for one of these (that labelled 3) is extremely unstable. Its concentration decreases on standing or on warming as seen in traces C and D. The other species that is responsible for the peak labeled 4 is the hydroxide complex $TPPFe^{III}OH$. This too is unstable and is eventually converted into the μ-oxo species, $TPPFe^{III}$–O–$Fe^{III}TPP$, as seen in trace E. The identity

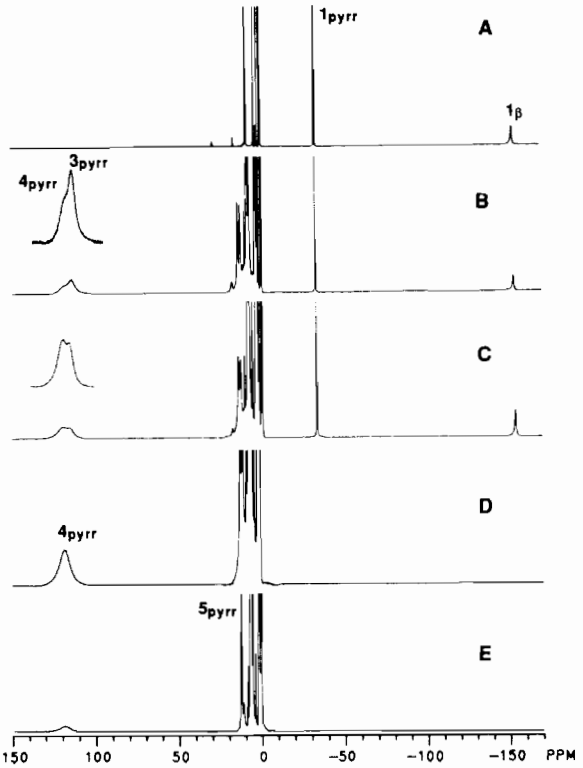

Fig. 3. 360 MHz ^2H NMR spectra obtained from the reaction between $TTPFe^{III}CH_2CH_3$ and O_2 at -70 °C in toluene-d_8 solution: (A) $TTPFe^{III}CH_2CH_3$ alone; (B, C) successive spectra run after the addition of dioxygen over a 2-h period with the sample in a -80 °C bath and recorded at -70 °C; (D) the sample after warming to -60 °C and cooling to -70 °C; (E) the sample after warming to room temperature and immediately cooling to -70 °C. Peaks of $TTPFe^{III}CH_2CH_3$ are labeled 1; those of $TTPFe^{III}OOCH_2CH_3$, 3; those of $TTPFe^{III}OH$, 4; and those of $TTPFe^{III}OFe^{III}TTP$, 5. Subscripts are used as given in Fig. 1. Reprinted with permission from ref. 43, copyright 1989 Am. Chem. Soc.

of $TPPFe^{III}OH$ is unambiguous since it can be prepared independently and is known to undergo dehydration to form the μ-oxo compound [44, 45].

In order to detect the presence of the ethyl peroxide ligand as the axial ligand, the oxygenation of specifically deuterated $TPPFe^{III}C_2D_5$ has been observed by ^2H NMR spectroscopy [41]. This technique has the advantage of producing narrower resonances and thereby it facilitates detection of resonances that are broad in the ^1H NMR spectrum. Figure 4 shows the spectrum of $TPPFe^{III}C_2D_5$ at -70 °C before the addition of dioxygen. The resonance of the methyl group of the axial ethyl group is labelled 1_β, the resonance of the methylene deuterons was not observed in this experiment, since it occurs at very low field. Trace B shows the effect of addition of dioxygen. Two new resonances, 3_α and 3_β, due to the methylene and methyl deuterons of the axial ethyl peroxide, appear in the spectrum. These resonances are clearly due to a paramagnetic

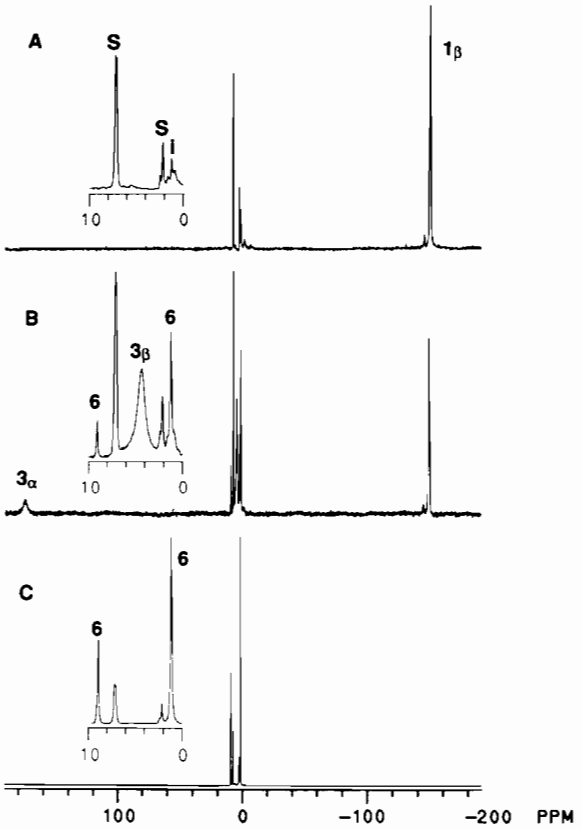

Fig. 4. 76 MHz ^2H NMR spectra obtained from the reaction of $TTPFe^{III}CD_2CD_3$ and O_2 at −70 °C in toluene solution: (A) $TTPFe^{III}CD_2CD_3$ alone; (B) the sample after the addition of O_2; (C) the same sample after 2 h. Insets show expansions of the 0–10 ppm region. Peaks of $TTPFeCD_2CD_3$ are labeled 1; those of $TTPFe^{III}OOCD_2CD_3$, 3; and those of acetaldehyde, 6. Subscripts α and β refer to methylene and methyl protons, respectively; i indicates an impurity. Reprinted with permission from ref. 43, copyright 1989 Am. Chem. Soc.

entity since they are broad and since the methylene resonance shows a large hyperfine shift. On standing, these resonances decay in intensity and are replaced with resonances (shown in trace C) which are due to acetylaldehyde. This is liberated from the ethyl peroxide complex via reaction (6).

$$PFe^{III}\text{–O–O–CHRR}' \longrightarrow PFe^{III}\text{–OH} + O{=}CRR' \quad (6)$$

Similar reactivity toward dioxygen has been observed with iron porphyrins bearing a range of axial ligands. Those with primary or secondary alkyl groups form alkyl peroxide complexes that fragment to produce aldehydes and ketones, respectively [41]. No other intermediates are observed during this process. Iron porphyrins with tertiary alkyl substituents are less stable than their primary or secondary alkyl counterparts due to steric crowding. However, these tertiary alkyl complexes can be prepared if suitable precautions are taken or the tertiary alkyl group is suitably modified [42]. They undergo a similar reaction with dioxygen via eqn. (4). With 4-camphane, a strained, caged hydrocarbon as the axial ligand, it has been possible to show that the tertiary alkyl peroxide complex undergoes homolytic fragmentation in non-polar media to form a six-coordinate ferryl intermediate via reaction (7).

$$py + PFe^{III}\text{–O–O–CR}_3 \longrightarrow (py)PFe^{IV}{=}O + {}^{\cdot}OCR_3 \quad (7)$$

Diamagnetic iron(II) alkyl complexes, $[PFe^{II}R]^-$, can be obtained by one-electron reduction of $PFe^{III}R$ [46]. These anions are diamagnetic complexes, and their alkyl groups are readily detected since the ring-current of the macrocycle shifts their NMR resonances upfield into the 0–8 ppm range. These iron(II) alkyl complexes do not undergo insertion of dioxygen into the Fe–C bond directly. Rather they are oxidized by dioxygen to the iron(III) form, $PFe^{III}R$, which then can undergo insertion of dioxygen as described above.

Iron(III) porphyrins with axial aryl ligands undergo complex oxidative processes that are highly dependent on reaction conditions [47]. With $PFe^{III}Ph$, the principal products are $[PFe^{IV}Ph]^+$ and $PFe^{III}Cl$ in chloroform or $PFe^{III}OPh$ in toluene. No direct evidence for the detection of an aryl peroxide intermediate has been found in these reactions. This is not at all surprising since aryl hydroperoxides are unknown species that are expected to rapidly decompose to form the phenoxide radical.

Experiments aimed at providing mechanistic information regarding the pathway of reaction (4) whereby the alkyl ligand is transformed into the alkylperoxide ligand through reaction with dioxygen are underway in our laboratory.

In toluene solution, iron porphyrins are unusually resistant to the bleaching by alkyl hydroperoxides and are effective catalysts for alkyl hydroperoxide destruction. In this non-polar solvent hydroxy iron(III) porphyrins catalyze the dehydration of alkyl peroxides that contain a hydrogen substituent on the α-carbon (eqn. (8)) [41, 48]. Thus ethyl hydroperoxide reacts with catalytic amounts of $TMPFe^{III}OH$ to form acetaldehyde through the simple two step process shown in Scheme 6. Low temperature ^1H NMR studies have

$$R_2CHOOH \longrightarrow R_2C{=}O + H_2O \quad (8)$$

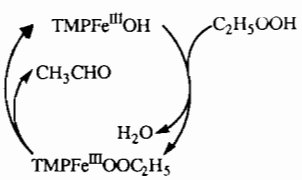

Scheme 6. Catalysis of hydroperoxide dehydration.

revealed the formation of $TMPFe^{III}OOC_2H_5$ in this process. This reaction, which results in dehydration rather than reduction of the peroxide, accounts for the variation of products obtained by the reaction of certain heme proteins with alkyl peroxides that bear α-hydrogens. Some proteins, particularly the peroxidases, catalytically reduce the peroxide to the alcohol and oxidize a second substrate while others (e.g. met myoglobin) or free heme cause catalytic dehydration [49].

The reaction of t-butyl hydroperoxide with iron porphyrins in toluene is more complex [43]. Treatment of either PFe^{II} or $PFe^{III}OH$ with excess t-butyl hydroperoxide at -70 °C results in the formation of detectable amounts of $PFe^{III}OOBu^t$. In the process t-butyl hydroperoxide is destroyed to give t-butyl alcohol, di-t-butyl peroxide, benzaldehyde, acetone, and benzyl t-butyl peroxide in an apparent free radical process. The formation of the alkyl peroxide complex from $PFe^{III}OH$ is likely to proceed via the steps in eqns. (9)–(12). The formation of the t-butyl hydroperoxy radical serves to initiate the free-radical decomposition of uncoordinated t-butyl hydroperoxide.

$$PFe^{II} + \text{t-BuOOH} \longrightarrow PFe^{III}OH + \text{t-BuO}^{\cdot} \quad (9)$$

$$\text{t-BuO}^{\cdot} + \text{t-BuOOH} \longrightarrow \text{t-BuOH} + \text{t-BuOO}^{\cdot} \quad (10)$$

$$PFe^{II} + \text{t-BuOO}^{\cdot} \longrightarrow PFe^{III}\text{–O–O–Bu}^t \quad (11)$$

$$PFe^{III}OH + \text{t-BuOOH} \longrightarrow PFe^{III}\text{–O–O–Bu}^t + H_2O \quad (12)$$

Once formed, Fe^{III}–O–O–Bu^t can serve as a source of ferryl complexes [42]. Warming a toluene solution of $TMPFe^{III}$–O–O–Bu^t produces the five-coordinate ferryl complex via homolytic cleavage, eqn. (13), while addition of an amine also induces homolytic cleavage to form the base stabilized ferryl complex by way of reaction (14).

$$TMPFe^{III}\text{–O–O–Bu}^t \xrightarrow{\text{warming}} TMPFe^{IV}=O + {}^{\cdot}OBu^t \quad (13)$$

$$TMPFe^{III}\text{–O–O–Bu}^t + \text{N-MeIm} \longrightarrow (\text{N-MeIm})TMPFe^{IV}=O + {}^{\cdot}OBu^t \quad (14)$$

The addition of t-butylhydroperoxide to $TMPFe^{II}$ has been used to generate solutions of $TMPFe^{III}$–O–O–Bu^t. The electronic absorption spectrum of this species consists of a Soret peak at 410 nm and weaker absorptions at 500, 570 and 680 nm [43]. It is important to note that this electronic spectrum did not show the equally intense, split Soret features (λ_{max} 330, 400 nm) that are characteristic of the recently reported compound **O** formed by horseradish peroxidase [4]. Thus the alkyl peroxide complexes described in this section do not appear to be models for this interesting enzyme intermediate.

The reactions of t-butyl hydroperoxide with iron porphyrins under different conditions than those used for the preceding studies produce two other species. Treatment of a dichloromethane solution of $PFe^{III}Cl$ and t-butyl hydroperoxide with choline in methanol at -79 °C followed by rapid freezing at 77 K produces a sample whose composition has been monitored by optical and EPR spectroscopy [50, 51]. These spectra reveal the formation of a set of low-spin ($S=1/2$), iron(III) complexes. One of these does not form when t-butyl hydroperoxide and the base, choline, are absent. This intermediate has been formulated as the six-coordinate $[PFe^{III}\text{–O–O–Bu}^t(OMe)]^-$. It should also be possible to obtain this low-spin species by the addition of methoxide to high-spin PFe–O–O–Bu^t, but that alternative route has not yet been pursued.

Addition of t-butyl hydroperoxide to $PFe^{III}Cl$ in dichloromethane at room temperature results in attack at a *meso* position of the porphyrin and formation of an iron(III) isoporphyrin complex as shown in eqn.

$$PFe^{III}Cl + t\text{-BuOOH} \longrightarrow \left[\begin{array}{c}\text{Ar}\\ \text{N}\quad\text{Cl}\quad\text{N}\\ \text{Ar}\quad\text{Fe}\quad\text{Ar}\\ \text{N}\quad\text{N}\quad\text{X}\\ \text{Ar}\end{array}\right]^+ \quad (15)$$

(15) [52]. The product is sufficiently stable so that it has been isolated presumably as the hydroxide salt. The identity of X has been assumed to be t-BuOO but it could just as well be t-BuO. The electronic absorption spectrum, which shows strong absorption in the near IR (895, 881 nm) and broad bands of reduced intensity in the Soret region (334, 450 nm), is clearly indicative of the formation of isoporphyrin. The ^1H NMR spectrum indicates the presence of high-spin iron(III) in a modified porphyrin with only mirror symmetry. Hence it has four pyrrole proton resonances in the 80–60 ppm region at 25 °C. The formation of this isoporphyrin may be a prelude to the process by which bleaching of porphyrins by hydroperoxides results in their destruction through opening up of the macrocyclic ring.

In order to provide more stable analogs for the very reactive iron/alkyl peroxide complexes formed in our laboratory, the reactivity of some main group analogs has been examined. Germanium(IV) complexes were chosen since these involve the metal in its highest oxidation state. Thus processes that might involve further oxidation of the metal ion were avoided. Scheme 7 summarizes the reactions that have been studied [53, 54].

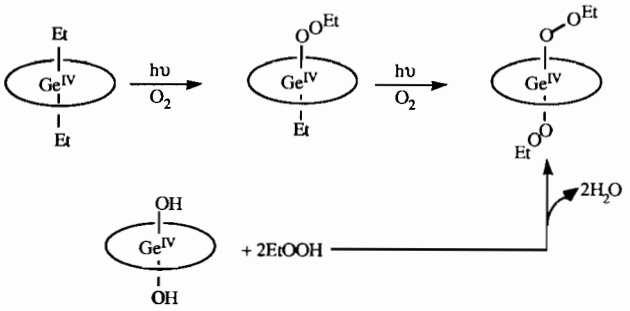

Scheme 7. Reactivity of stable germanium porphyrin models.

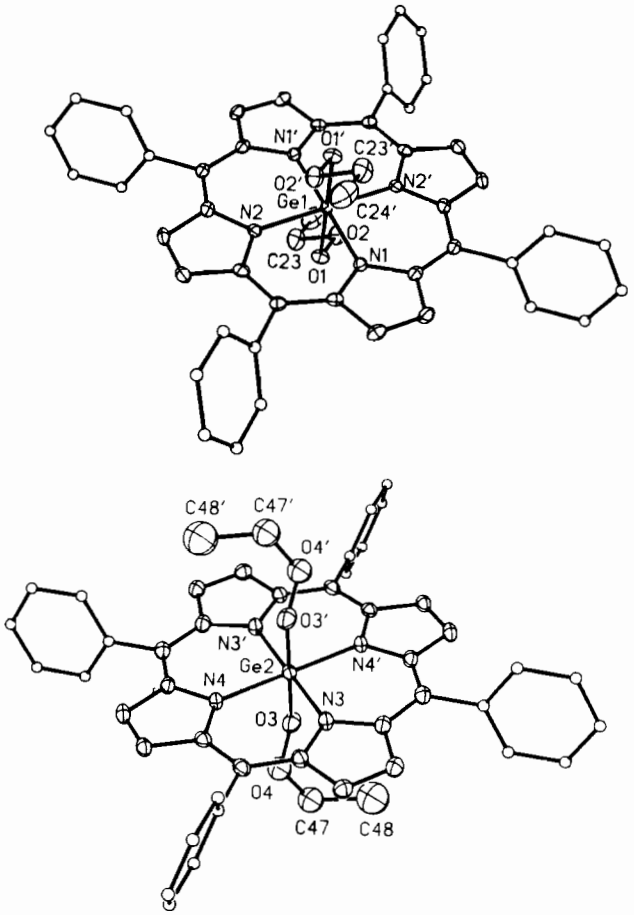

Fig. 5. A perspective view of TPPGe^{IV}(OOCH$_2$CH$_3$)$_2$, a model for PFe^{III}–O–O–R: (top) the ordered molecule and (bottom) the molecule that shows disorder in the ethyl peroxide ligand with the principal form (54.8% occupancy) shown. Reprinted with permission from ref. 54, copyright 1990 Am. Chem. Soc.

Solutions of PFe^{IV}Et$_2$, unlike solutions of PFe^{III}Et, are stable to dioxygen, even at 25 °C, unless they are exposed to light. Photolysis in the presence of dioxygen induces stepwise conversion of PGe^{IV}Et$_2$ to PGe^{IV}(OOEt)Et and to PGe^{IV}(OOEt)$_2$. Presumably this occurs via photolytic homolysis of the Ge–C bonds. PGe^{IV}(OOEt)$_2$ can also be formed by the addition of ethyl hydroperoxide to PGe^{IV}(OH)$_2$. These reactions which form the ethyl peroxide complexes of germanium are clearly related to reactions (4) and (5) which lead to the formation of the much more reactive PFe^{III}OOEt. In contrast to this iron complex, which cannot be observed above −70 °C, PGe^{IV}(OOEt)$_2$ is sufficiently stable so that it can be handled at room temperature and readily isolated. The results of an X-ray diffraction study of TPPGe^{IV}(OOEt)$_2$ are shown in Fig. 5 [54]. The compound crystallizes with two different molecules in the asymmetric unit. Each molecule is centrosymmetric with two axial ethyl peroxide ligands. The conformation of these axial ligands differs in the two molecules. We believe that the coordination of the ethyl peroxide unit in PFe^{III}–O–O–R is similar to that seen in this stable germanium peroxide complex. However, the iron complex is five-coordinate with the iron ion out of the porphyrin plane.

Conclusions

Over the last fifteen years considerable attention has been given to identifying the forms of metalloporphyrins, and particularly iron porphyrins, that are responsible for the oxidation of organic substrates [55, 56]. An important component of that work has been experiments designed to directly detect reactive intermediates by spectroscopic means. Here I have reviewed work that has uncovered the existence of three iron complexes containing the peroxide link: PFe^{III}–O–O–Fe^{III}P, [PFeO$_2$]$^-$ and PFe^{III}–O–O–R. Considerable progress has been made in understanding the chemical behavior of these species. A particularly significant aspect of that is their conversion into complexes containing the ferryl moiety, [Fe^{IV}=O]$^{2+}$, which appears in many cases to the species ultimately responsible for transfer of an oxygen atom to a suitable receptor. In that regard, efforts to convert [PFeO$_2$]$^-$ into a ferryl complex, a goal which has not been achieved, seems particularly worthwhile. Attempts to interrelate the chemistry of [PFeO$_2$]$^-$ to other intermediates such as PFe^{III}–O–O–Fe^{III}P, PFe^{III}–O–O–R and PFe^{IV}=O will have to contend with problems regarding the suitability of various solvents. While [PFeO$_2$]$^-$ is generally prepared in polar and potentially coordinating solvents, the other intermediates are usually handled in solvents of low polarity and low coordinating ability.

A number of non-heme iron proteins, hemerythrin, ribonucleotide reductase and methane monoxygenase, react with and activate dioxygen [57]. These are also likely to form iron–peroxo complexes. As more attention is focused on these non-heme iron enzymes and their models, more will be learned about iron–peroxide coordination and activation. There are already several

interesting intermediates that have been spectroscopically detected with non-heme iron models [57].

Acknowledgements

I thank the NIH (grant GM26226) for financial support, my long term collaborators, Professor G. N. La Mar, Professor L. Latos-Grażyński and Dr M. M. Olmstead for their countless contributions, my former students D. H. Chin, R. J. Cheng, M. W. Renner, R. D. Arasasingham, C. R. Cornman, N. Safari and R. L. Hart, for their enthusiastic assistance, and Professor J. S. Valentine for a helpful discussion and a copy of ref. 36.

References

1 J. Everse, K. E. Everse and M. B. Grisham (eds.), *Peroxidases in Chemistry and Biology,* Vols. 1 and 2, CRC Press, Boca Raton, FL, 1991.
2 H. B. Dunford and J. S. Stillman, *Coord. Chem. Rev., 19* (1976) 187.
3 V. Thanabal, J. S. de Ropp and G. N. La Mar, *J. Am. Chem. Soc., 110* (1988) 3027.
4 H. K. Back and H. E. Van Wart, *Biochemistry, 28* (1989) 5714.
5 P. R. Ortiz de Montellano, (ed.), *Cytochrome P450,* Plenum, New York, 1986.
6 J. H. Dawson, *Chem. Rev., 87* (1987) 1255.
7 P. R. Ortiz de Montellano, *Acc. Chem. Res., 20* (1987) 289.
8 P. A. Cole, C. H. Robinson, *J. Am. Chem. Soc., 113* (1991), 8130.
9 T. G. Traylor, W. A. Lee, D. V. Stynes, *J. Am. Chem. Soc., 106* (1984) 755.
10 G. N. La Mar and F. A. Walker (Jensen), in D. Dolphin (ed.), *The Porphyrins,* Vol. 4, Academic Press, New York, 1979, p. 61.
11 L. Latos-Grażyński, A. L. Balch and G. N. La Mar, in K. Kadish (ed.), *Electrochemical and Spectroscopic Studies of Biological Redox Components,* Advances in Chemistry, Vol. 201, American Chemical Society, Washington, DC, 1982, p. 661.
12 H. M. Goff, in A. P. B. Lever and H. B. Gray (eds.), *Iron Porphyrins,* Part I, Addison-Wesley, London, 1983, p. 327.
13 T. G. Traylor and F. Xu, *J. Am. Chem. Soc., 112* (1990) 178, and refs. therein.
14 T. C. Bruice, *Acc. Chem. Res., 24* (1991) 243, and refs. therein.
15 D.-H. Chin, J. Del Gaudio, G. N. La Mar and A. L. Balch, *J. Am. Chem. Soc., 99* (1977) 5486.
16 D.-H. Chin, G. N. La Mar and A. L. Balch, *J. Am. Chem. Soc., 102* (1980) 4344.
17 G. N. La Mar, J. S. de Ropp, L. Latos-Grażyński, A. L. Balch, R. B. Johnson, K. M. Smith, D. W. Parish and R.-J. Cheng, *J. Am. Chem. Soc., 105* (1983) 782.
18 G. Simonneaux, W. F. Scholz, C. A. Reed and G. Lang, *Biochim. Biophys. Acta, 716* (1982) 1.
19 Y. Mizutani, S. Hashimoto, Y. Tatsuno and T. Kitagawa, *J. Am. Chem. Soc., 112* (1990) 6809.
20 G. N. La Mar, G. R. Eaton, R. H. Holm and F. A. Walker, *J. Am. Chem. Soc., 95* (1973) 63.
21 K. S. Murray, *Coord. Chem. Rev., 12* (1974) 1.
22 D.-H. Chin, G. N. La Mar and A. L. Balch, *J. Am. Chem. Soc., 102* (1980) 5945.
23 D.-H. Chin, G. N. La Mar and A. L. Balch, *J. Am. Chem. Soc., 102* (1980) 1446.
24 A. L. Balch, Y. W. Chan, R.-J. Cheng, G. N. La Mar, L. Latos-Grażyński and M. W. Renner, *J. Am. Chem. Soc., 106* (1984) 7779.
25 J. E. Penner-Hahn, T. J. McMurry, M. W. Renner, L. Latos-Grażyński, K. S. Eble, I. M. Davis, A. L. Balch, J. T. Groves, J. H. Dawson and K. O. Hodgson, *J. Biol. Chem., 258* (1983) 12761.
26 A. R. Miksztal and J. S. Valentine, *Inorg. Chem., 23* (1984) 3548.
27 L. Latos-Grażyński, R.-J. Cheng, G. N. La Mar and A. L. Balch, *J. Am. Chem. Soc., 104* (1982) 5992.
28 I. R. Paeng, H. Shiwaku and K. Nakamoto, *J. Am. Chem. Soc., 110* (1988) 1995.
29 I. R. Paeng and K. Nakamoto, *J. Am. Chem. Soc., 112* (1990) 3289.
30 J. S. Valentine and E. McCandlish, *Front. Biol. Energ., 2* (1978) 933.
31 E. McCandlish, A. R. Miksztal, M. Nappa, A. Q. Sprenger, J. S. Valentine, J. D. Strong and T. G. Spiro, *J. Am. Chem. Soc., 102* (1980) 4268.
32 J. N. Burstyn, J. A. Roe, A. R. Miksztal, B. A. Shaevitz, G. Lang and J. S. Valentine, *J. Am. Chem. Soc., 110* (1988) 1382.
33 A. Shirazi and H. M. Goff, *J. Am. Chem. Soc., 104* (1982) 6318.
34 C. A. Reed, in K. Kadish (ed.), *Electrochemical and Spectroscopic Studies of Biological Redox Components,* Advances in Chemistry, Vol. 201, American Chemical Society, Washington, DC, 1982, p. 333.
35 C. H. Welborn, D. Dolphin and B. R. James, *J. Am. Chem. Soc., 103* (1981) 2869.
36 J. N. Burstyn, *Ph. D. Thesis,* University of California, Los Angeles, 1986, p. 89.
37 R. Friant, J. Goulon, J. Fischer, L. Ricard, M. Schappacher, R. Weiss and M. Momenteau, *Nouv. J. Chim., 9* (1985) 33.
38 R. Guilard, J. M. Latour, C. Lecomte, J. C. Marchon, J. Protas and D. Ripoll, *Inorg. Chem., 17* (1978) 1228.
39 R. B. VanAtta, C. E. Strouse, L. K. Hanson and J. S. Valentine, *J. Am. Chem. Soc., 109* (1987) 1425.
40 R. D. Arasasingham, A. L. Balch and L. Latos-Grażyński, *J. Am. Chem. Soc., 109* (1987) 5846.
41 R. D. Arasasingham, A. L. Balch, C. R. Cornman and L. Latos-Grażyński, *J. Am. Chem. Soc., 111* (1989) 4357.
42 A. L. Balch, R. L. Hart, L. Latos-Grażyński and T. G. Traylor, *J. Am. Chem. Soc., 112* (1990) 7382.
43 R. D. Arasasingham. C. R. Cornman and A. L. Balch, *J. Am. Chem. Soc., 111* (1989) 7800.
44 R.-J. Cheng, L. Latos-Grażyński and A. L. Balch, *Inorg. Chem., 22* (1982) 2412.
45 L. Fielding, G. R. Eaton and S. S. Eaton, *Inorg. Chem., 24* (1985) 2309.
46 A. L. Balch, C. R. Cornman, N. Safari and L. Latos-Grażyński, *Organometallics, 9* (1990) 2420.
47 R. D. Arasasingham, A. L. Balch, R. L. Hart and L. Latos-Grażyński, *J. Am. Chem. Soc., 112*(1990) 7566.
48 R. Labeque and L. J. Marnett, *J. Am. Chem. Soc., 111* (1989) 6621.
49 L. J. Marnett, P. Weller and J. R. Batista, in P. Ortiz de Montellano (ed.), *Cytochrome P-450: Structure, Mechanism and Function,* Plenum, New York, 1986, p. 29.

50 K. Tajima, J. Jinno, K. Ishizu, H. Sakurai and H. Ohya-Nishiguchi, *Inorg. Chem., 28* (1989) 709.
51 K. Tajima, M. Shigematsu, J. Jinno, K. Ishizu and H. Ohya-Nishiguchi, *J. Chem. Soc., Chem. Commun.,* (1990) 144.
52 A. Gold, W. Ivey, G. E. Toney and R. Sangaiah, *Inorg. Chem., 23* (1984) 2932.
53 C. Cloutour, D. La Farque, J. A. Richards and J.-C. Pommier, *J. Organomet. Chem., 137* (1977) 157.
54 A. L. Balch, C. R. Cornman and M. M. Olmstead, *J. Am. Chem. Soc., 112* (1990) 2963.
55 B. Meunier, *Bull. Soc. Chim. Fr.,* (1986) 578.
56 J. T. Groves, *J. Chem. Educ., 62* (1985) 928.
57 L. Que, Jr. and A. E. True, *Prog. Inorg. Chem., 38* (1990) 97.